Paper No. DS1-T3-1, pp. 1-4

18th INTERNATIONAL SYMPOSIUM on POWER ELECTRONICS - Ee 2015

NOVI SAD, SERBIA, October 28th- 30th, 2015

MCCA MODEL OF ASYMMETRICAL SIX-PHASE INDUCTION MACHINE

Dejan Jerkan*, Dragan Milićević*, Vladimir Katić*, Marian Greconici**

*University of Novi Sad, Faculty of Technical Sciences, Novi Sad, Serbia

**Universitatea Politehnica din Timisoara, Timisoara, Romania

Abstract: *Multi-phase squirrel-cage induction machines (IM) are showing good prospect in electrical vehicle's propulsion systems because of their numerous advantages. Asymmetrical six-phase IM is one of the most popular choices for such drives; particularly because its stator windings are consisting of two three-phase systems that are independently connected in two different star connections (symmetrical six-phase machine has one star connection for all stator windings). In this paper authors are suggesting multiple-coupled circuit approach (MCCA) for machine modeling, and inductance matrix of the machine is obtained from series of magneto-static two-dimensional finite element method (2D-FEA) simulations, which are more simple and faster than time-stepping 2D-FEA approaches. Results of proposed model are verified through computer simulations.*

Key Words: Asymmetrical six-phaseIM, 2D-FEA, MCCA.

1. INTRODUCTION

Multi-phase IMs are very popular in recent years, especially in drives designed for application in electrical vehicle's systems [1]. Modern power electronic converters are able to generate adequate multi-phase system of voltages (as a single unit, or combining more than one three-phase inverters), which was major setback for wide usage of multi-phase machines earlier [2]. When machine is designed to have more stator phase windings (more than traditional three as in three-phase systems), possible failure in one stator phase is not so severe fault as it is in classical three-phase machines, and output power and torque of such drives will not suffer significantly, making these drives more robust and reliable.

In order to investigate behavior of such multi-phase systems, adequate mathematical model of the machine is necessary. Modeling of asymmetrical six-phase machine in commercial software implementing FEA is very hard and time consuming (these software's are not allowing definition of more than one neutral point for star connection of the windings). MCCA is alternative method for this purpose. It is less time-consuming and easier for analytical investigation of energy conversion phenomena, but major problem of this method is how to obtain inductance matrix of analyzed machine. Winding function approach (WFA) and modified winding function approach (MWFA) are offering solution for this problem [4], but these approaches don't possess sufficient precision, because variations of air-gap width due to stator and rotor slots cannot be accounted for with satisfying precision.

In a research for the purpose of this paper, authors used series of magneto-static FEA simulations in order to obtain inductance matrix of the machine. Magneto-static 2D-FEA simulations are the simplest simulations, and they can be carried out very fast, especially when linear materials are used. Results of the simulations are then represented with Fourier series and incorporated in MCCA model. Numerical simulations are used for verification of the proposed model.

2. MAGNETO-STATIC FEA MODEL OF ASSYMETRICAL SIX-PHASE MACHINE

As mentioned in Chapter 1, magneto-static 2D-FEA simulations are the least resource-demanding calculations. Excitation in these models comes from permanent magnets or DC current sources. It can be used for static inductance calculations, but IMs have time and position varying inductances, so it is necessary to perform series of simulations for different rotor positions in order to obtain complete matrix as a function of rotor angular position.

2D-FEA algorithms implemented for the purpose of electrical machine's analysis are based on the evaluation of the z component of the magnetic vector potential A(under assumption that cross-section of the machine is located in xy plane), calculated over domain of interest that is divided into triangular segments, called finite elements (division of that domain on finite elements is called meshing). For each node of the segment, equation (1) can be written:

$$-\frac{\partial}{\partial x}\left(\frac{1}{\mu}\left(\frac{\partial A_z}{\partial x}\right)\right)-\frac{\partial}{\partial y}\left(\frac{1}{\mu}\left(\frac{\partial A_z}{\partial y}\right)\right)=J_s, \qquad (1)$$

where μ is the permeability of the material, and $J_s$represents current density vector.After finding values of A_z in all nodes of meshed region, calculating flux linkages of specific phase windings can be done. The flux linkage Ψ_{ij} of the j-th winding when the i-th winding is supplied with current can be expressed by [5]:

$$\Psi_{ij} = p\frac{1}{S_j}\left(\int_{\Omega_j^+} A_z d\Omega - \int_{\Omega_j^-} A_z d\Omega\right) N_j l_j, \qquad (2)$$

where p is number of pole pairs N_j is the number of turns of j-th winding, l_j is the length of the stator core and S_j is the cross-section of the coil region. Ω_j^+ and Ω_j^- represent the positive and negative trace of the winding in xy plane. Now it is possible to calculate all inductances in IM as a function of rotor position. Starting from a reference position of the rotor, a stator phase or a rotor loop is supplied with unity current at a time so each self and mutual inductance is equal to the linkage flux. Figure 1 shows flux distribution in axial cross section of the machine for this case. The rotor is turn by an angular fraction and a new FEA is carried out.

Periodic nature of inductances in IM allows reduction of necessary field calculations. It is sufficient to evaluate waveforms of self and mutual inductances as the function of the rotor position of one rotor loop and one stator phase. Other inductances can be obtained from these simulations using phase shift and symmetry of the machine. In figure 3 is shown mutual inductance between stator phase a and rotor loop 1 as a function of electrical rotor angle ϑ, and in figure 4 is shown its spectra. Shape of stator-rotor inductances is determined with stator winding distribution, number of pole pairs and number of phases. Because stator winding is made of two different star-connected three-phase windings shifted for 30°, stator-stator mutual inductances are not all equal. Mutual inductances within the same winding are all the same, but because asymmetrical position of another winding, some phases theoretically should not have any mutual coupling [6] (please see figures 2 and 5, where connection of phase windings and induced voltage phasor diagrams are shown). Mutual inductances M_{af} ,M_{bc} and M_{de} should be equal to zero, but due to imperfections in machine's magnetic circuit (mostly because existence of stator and rotor slots that are changing the flux paths and flux leakage) this is not the case. In figure 6 are shown inductances concerning phase a, and in zoomed part of the figure one may notice small fluctuation around zero value of the inductance M_{af}. Also, fluctuation of other inductances can be seen, and explanation for these phenomena is the same.

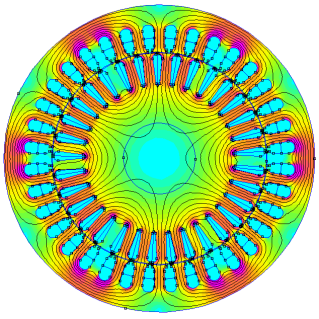

Fig. 1. *Flux distribution in axial cross section of the machine*

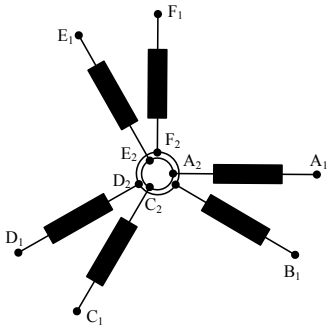

Fig. 2. *Connection of stator windings*

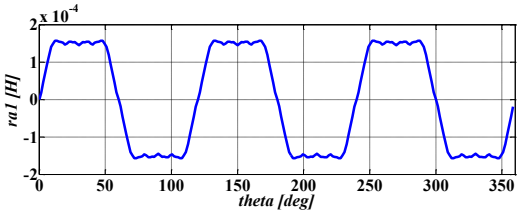

Fig. 3. *Mutual inductance between stator phase a and rotorloop 1 as a function of electrical rotor angle.M_{ar1}=M_{ar1}(ϑ)*

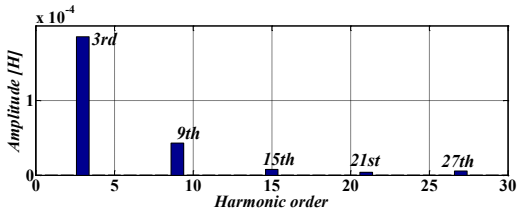

Fig. 4. *Spectra of mutual inductance M_{ar1}*

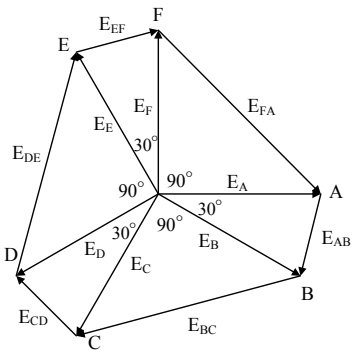

Fig. 5. *Induced voltages phasor diagram*

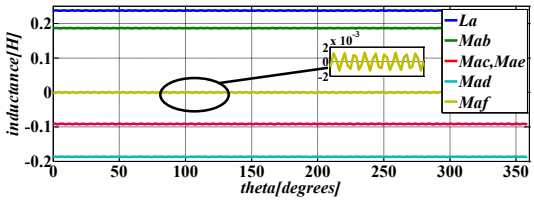

Fig. 6. *Stator inductances*

3. MCCA MODEL OF THE MACHINE

MCCA model of the machine [8] is based on circuit equations of voltage balance. Circuits in electrical

machine are coupled magnetically, and because of variation of their mutual position inductance matrix is complex function of machine's geometry and rotor position. Matrix equation 3.1 incorporates all electrical circuits in IM, both stator phases and rotor loops (number of rotor loops is equal to number of rotor bars N_B), and in equations 3.2-3.9 are defined all vectors and sub-matrices used in this equation. Stator-stator and rotor-rotor inductance matrices $\boldsymbol{L_{ss}}$ and $\boldsymbol{L_{rr}}$ can be considered as constant if their small variation as a result of slotting is not of interest, while stator-rotor and rotor-stator matrices ($\boldsymbol{L_{sr}}$ and $\boldsymbol{L_{rs}}$) are always periodic functions of rotor electrical rotor angle ϑ. As shown in figure 3, these matrices are complex periodic functions, but they can be represented with their fundamental harmonic components, if necessary.

$$\begin{bmatrix}\boldsymbol{U_s}\\ \boldsymbol{U_r}\end{bmatrix} = \left(\begin{bmatrix}\boldsymbol{R_{ss}} & \\ & \boldsymbol{R_{rr}}\end{bmatrix} + \frac{d}{dt}\begin{bmatrix}\boldsymbol{L_{ss}} & \boldsymbol{L_{sr}}\\ \boldsymbol{L_{rs}} & \boldsymbol{L_{rr}}\end{bmatrix}\right)\begin{bmatrix}\boldsymbol{I_s}\\ \boldsymbol{I_r}\end{bmatrix} \quad (3.1)$$

$$\boldsymbol{U_s} = [U_a \quad U_b \quad U_c \quad U_d \quad U_e \quad U_f]^T \quad (3.2)$$

$$\boldsymbol{U_r} = [0 \quad \dots \quad 0]^T_{N_B} \quad (3.3)$$

$$\boldsymbol{I_s} = [I_a \quad I_b \quad I_c \quad I_d \quad I_e \quad I_f]^T \quad (3.4)$$

$$\boldsymbol{I_r} = [I_{r1} \quad \dots \quad I_{rN_B}]^T_{N_B} \quad (3.5)$$

$$\boldsymbol{R_{ss}} = diag(R_s \quad R_s \quad R_s \quad R_s \quad R_s \quad R_s) \quad (3.6)$$

$$\boldsymbol{R_{rr}} = diag(R_r \quad \dots \quad R_r)_{N_B} \quad (3.7)$$

$$\boldsymbol{L_{ss}} = \begin{bmatrix} L_a & M_{ab} & M_{ac} & M_{ad} & M_{ae} & M_{af}\\ M_{ba} & L_b & M_{bc} & M_{bd} & M_{be} & M_{bf}\\ M_{ca} & M_{cb} & L_c & M_{cd} & M_{ce} & M_{cf}\\ M_{da} & M_{db} & M_{dc} & L_d & M_{de} & M_{df}\\ M_{ea} & M_{eb} & M_{ec} & M_{ed} & L_e & M_{ef}\\ M_{fa} & M_{fb} & M_{fc} & M_{fd} & M_{fe} & L_f \end{bmatrix} \quad (3.7)$$

$$\boldsymbol{L_{sr}} = \begin{bmatrix} M_{ar_1} & M_{ar_2} & \dots & M_{ar_{N_B-1}} & M_{ar_{N_B}}\\ M_{br_1} & M_{br_2} & \dots & M_{br_{N_B-1}} & M_{br_{N_B}}\\ M_{cr_1} & M_{cr_2} & \dots & M_{cr_{N_B-1}} & M_{cr_{N_B}}\\ M_{dr_1} & M_{dr_2} & \dots & M_{dr_{N_B-1}} & M_{dr_{N_B}}\\ M_{er_1} & M_{er_2} & \dots & M_{er_{N_B-1}} & M_{er_{N_B}}\\ M_{fr_1} & M_{fr_2} & \dots & M_{fr_{N_B-1}} & M_{fr_{N_B}} \end{bmatrix}_{6xN_B} = \boldsymbol{L_{rs}^T} \quad (3.8)$$

$$\boldsymbol{L_{rr}} = \begin{bmatrix} L_{r_1} & M_{r_{12}} & \dots & M_{r_{1N_B-1}} & M_{r_{1N_B}}\\ M_{r_{21}} & L_{r_2} & \dots & M_{r_{2N_B-1}} & M_{r_{2N_B}}\\ \vdots & \vdots & \dots & \vdots & \vdots\\ \vdots & \vdots & \dots & \vdots & \vdots\\ M_{r_{(N_B-1)1}} & 0 & \dots & L_{r_{N_B-1}} & M_{r_{(N_B-1)N_B}}\\ M_{r_{N_B1}} & M_{r_{N_B2}} & \dots & M_{r_{N_BN_B-1}} & L_{r_{N_B}} \end{bmatrix}_{N_BxN_B} \quad (3.9)$$

Torque generation in MCCA model of the IM is modeled using virtual work principle. All sub-matrices are function of rotor angular position, so they all participate in torque generation.

$$T_e = \frac{1}{2}p\begin{bmatrix}\boldsymbol{I_s}\\ \boldsymbol{I_r}\end{bmatrix}^T \frac{d}{d\vartheta}\left(\begin{bmatrix}\boldsymbol{L_{ss}} & \boldsymbol{L_{sr}}\\ \boldsymbol{L_{rs}} & \boldsymbol{L_{rr}}\end{bmatrix}\right)\begin{bmatrix}\boldsymbol{I_s}\\ \boldsymbol{I_r}\end{bmatrix} \quad (4)$$

4. SIMULATION RESULTS

In this chapter are presented some characteristic results of simulations conducted on developed MCCA model of the IM. In figure 6 are shown applied asymmetrical voltages (rated voltage of the machine is 220V RMS)

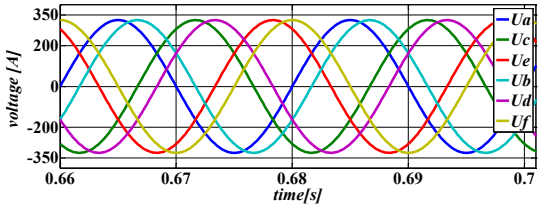

Fig 7.*Applied asymmetrical voltages*

In figures 8 and 9 are shown developed torque and mechanical speed during start of unloaded machine, respectively. MCCA model with inductance matrices variation included is very detail representation of the machine, so there are more fluctuations in torque and speed during transients, due to parasitic high-order torque components [9].

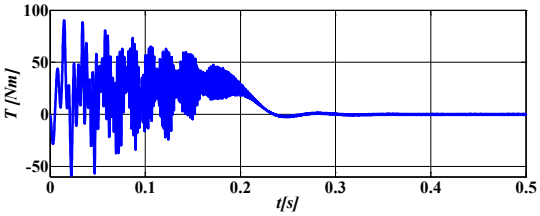

Fig. 8. *Developed torque during start of unloaded machine*

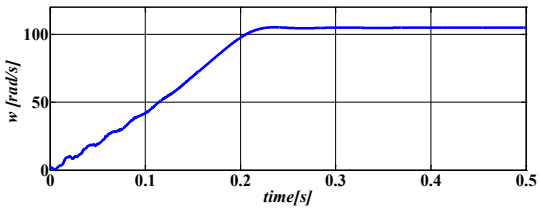

Fig. 9. *Mechanical speed during start of unloaded machine*

Higher order harmonic components in inductance matrices are causing higher order harmonics in stator currents [11], even when the machine is supplied with ideally sinusoidal voltages, which can be observed in figure 10, where all six stator currents are shown.

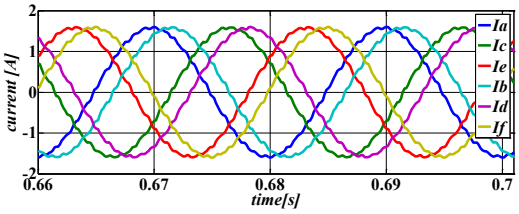

Fig. 10. *Stator currents of unloaded IM*

Similar results for loaded IM can be seen on figures 11-13, where developed torque, mechanical speed and stator currents are shown respectively. IM is loaded with rated torque of *11.3 Nm* at *t=0.35s*.

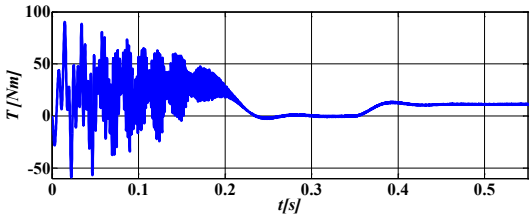

Fig. 11. *Developed torque during start of IM loaded at t=0.35s*

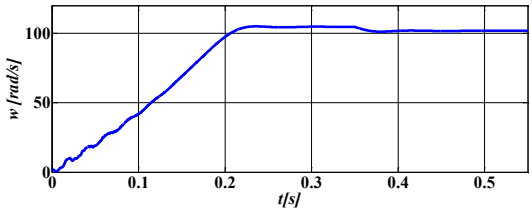

Fig. 12. *Mechanical speed during start of IM loaded at t=0.35s*

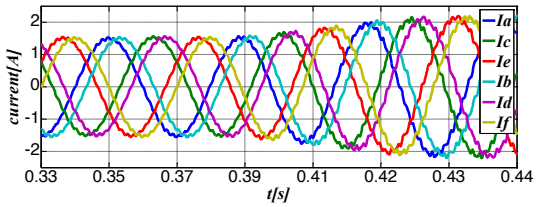

Fig. 13. *Stator currents of IM loaded at t=0.35s*

ACKNOWLEDGMENT

This work was supported by the Ministry of Education, Science and Technological Development of the Republic of Serbia under project III42004.

5. REFERENCES

[1] E. Levi, R. Bojoi, F. Profumo, H. A. Toliyat, and S. Williamson, "Multiphase induction motor drives – a technology status review," *IET Electr. Power Appl.*, vol. 1, no. 4, p. 489, 2007.

[2] L. De Camillis, M. Matuonto, A. Monti, and A. Vignati, "Optimizing current control performance in double winding asynchronous motors in large power inverter drives," *IEEE Trans. Power Electron.*, vol. 16, no. 5, pp. 676–685, Sep. 2001.

[3] M. Jones and L. Emil, "A literature survey of state-of-the-art in multiphase AC drives," in *37th Int. Universities Power Engineering Conference UPEC*, 2002, pp. 505–510.

[4] Joksimovic, G.; Djurovic, M; Penman, J., "Cage rotor MMF: Winding Function Approach,"*Power Engineering Review, IEEE*, Vol. 21, No. 4, 64-66.April 2001.

[5] P. Silvester, "Finite Elements for Electrical Engineers", Cambridge University Press, 1990.

[6] R. Nelson and P. Krause, "Induction Machine Analysis for Arbitrary Displacement Between Multiple Winding Sets," *IEEE Trans. Power Appar. Syst.*, vol. PAS-93, no. 3, pp. 841–848, May 1974.

[7] D. Hadiouche, H. Razik, and A. Rezzoug, "Modelling of a double-star induction motor with an arbitrary shift angle between its three phase windings," in *Proc. 9th Int. Conf. on Power Electronics and Motion Control PEMC*, Kosice, Slovakia, 2000, pp. 5.125–5.130.

[8] Luo, X.; Liao, Y.; Toliyat, H.A.; El-Antably A.; Lipo, T.A., "Multiple Coupled Circuit Modeling of Induction Machines," *IEEE Transactions Industry Applications*, Vol. 31, No. 2, pp. 311-318, 1995.

[9] S. Williamson and S. Smith, "Pulsating torque and losses in multiphase induction machines," *IEEE Trans. Ind. Appl.*, vol. 39, no. 4, pp. 986–993, Jul. 2003.

[10] A. N. Golubev and S. V. Ignatenko, "Influence of number of stator-winding phases on the noise characteristics of an asynchronous motor," *Russ. Electr. Eng.*, vol. 71, pp. 41–46, 2000.

[11] S.Z. Jiang, K. T. Chau, and C. C. Chan, "Spectral analysis of a new six-phase pole-changing induction motor drive for electric vehicles," *IEEE Trans. Ind. Electron.*, vol. 50, no. 1, pp. 123–131, Feb. 2003.